

Electronic Supplementary Information

Direct Route of Ultrafast Charge-Pair Generation Upon Below-Band-Gap Excitation in P3HT: Effect of External Electric Field

Debkumar Rana^{†*}, Ayush Kant Ranga, Arnulf Materny^{*}

School of Science, Constructor University, Campus Ring 1, 28759 Bremen, Germany

*Corresponding authors: debkumar.rana@mbi-berlin.de; amaterny@constructor.university

[†]Present affiliation: Max Born Institut für Nichtlineare Optik und Kurzzeitspektroskopie,
Max Born Strasse 2A, 12489 Berlin, Germany

1. UV-Vis Absorption of P3HT

The UV-Vis absorption of neat P3HT thin film is shown in Fig. S1. The regioregular P3HT thin film shows a broad absorption from 365 nm to 680 nm with three distinct features at 507, 553 and 598 nm. The spin-cast thin film shows the characteristic transitions related to inter-chain exciton delocalization and a significant coupling to vibrations. The ratio of the amplitudes of the A_{0-0} (598 nm) and the A_{0-1} (553 nm) peaks is characteristic for partially ordered H-aggregate-like chains coexisting with non-aggregated chain sequences. The absorption strength on the higher wavelength side after 620 nm is extremely low, but not zero.

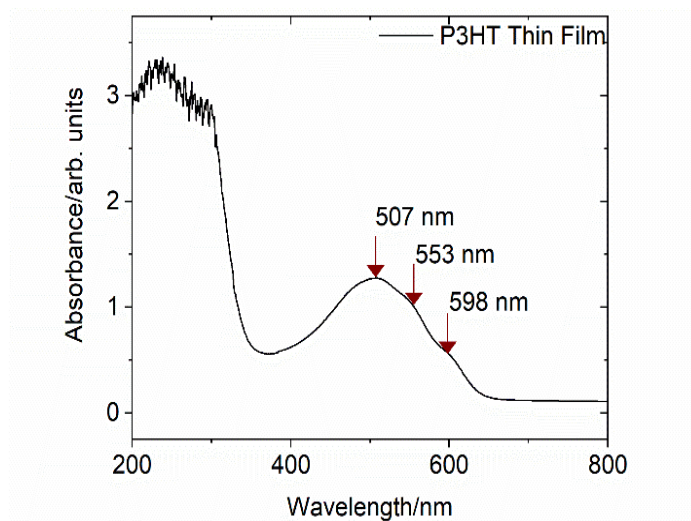


Fig. S1 UV-Vis absorption spectrum of the neat P3HT thin film.

2. IV Characteristics of P3HT-Only Diode

The arrangement of the P3HT-only diode shown in Fig. S2 allows for the application of an external electric field. The asymmetry of the layers results in an internal field of -0.8 V.

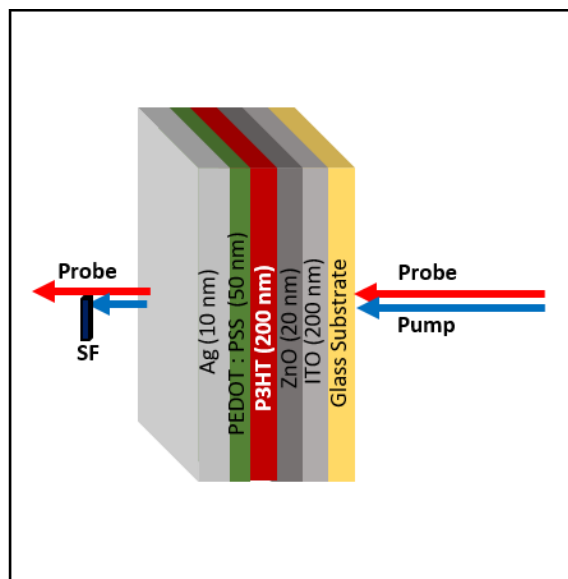


Fig. S2 P3HT device structure.

Figure S3 shows the current-voltage (I - V) characteristics of the P3HT device measured in the dark and when light is shining on it. An illumination with an air mass 1.5 sun spectrum, which is equivalent to a power density of 100 mW cm^{-2} was used for the measurement under light.

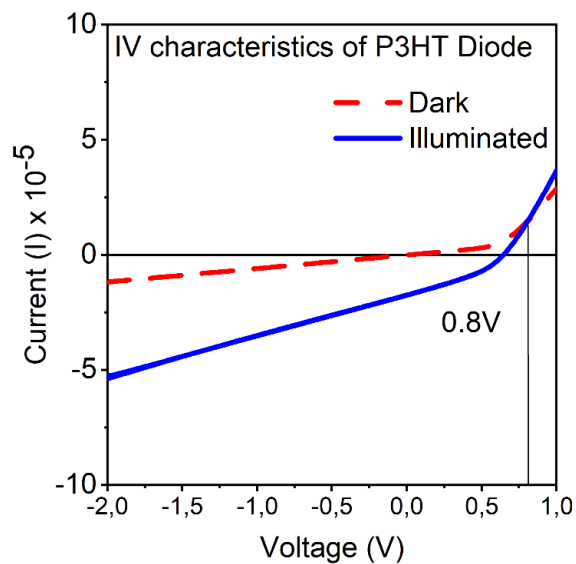


Fig. S3 I-V characteristics of the P3HT diode.

3. Transient at 520 nm Excitation

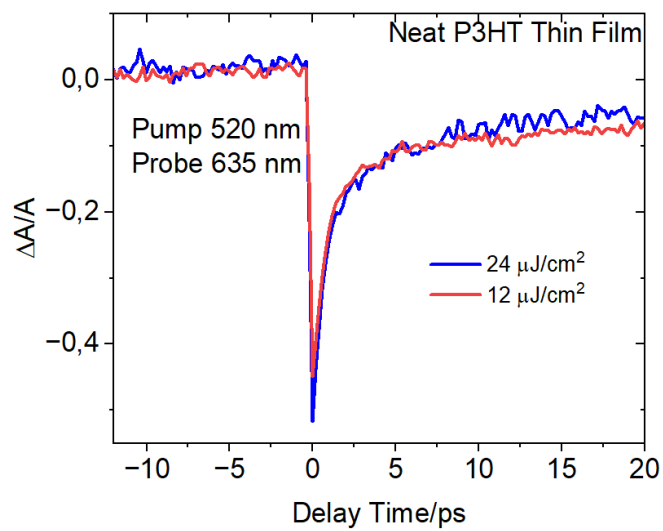


Fig. S4 Differential transient transmission dynamics ($\Delta T/T$) obtained from the neat P3HT thin film probing the polaron pair dynamics at 635 nm after 520 nm excitation with two different fluences.

4. Fitting Results

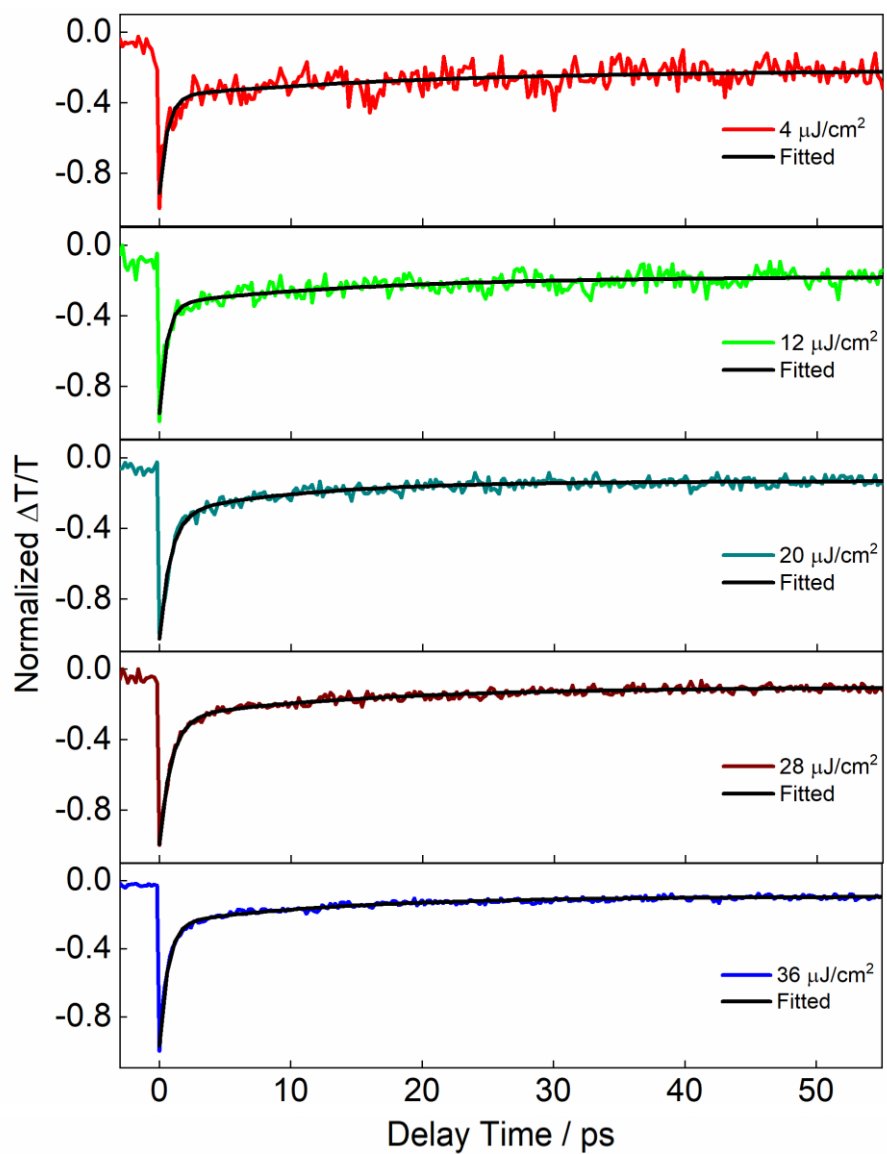


Fig. S5 Fitting results using the exponential model for the differential transient transmission dynamics ($\Delta T/T$) obtained from the neat P3HT thin film at different excitation fluences where pump and probe both were at 638 nm.

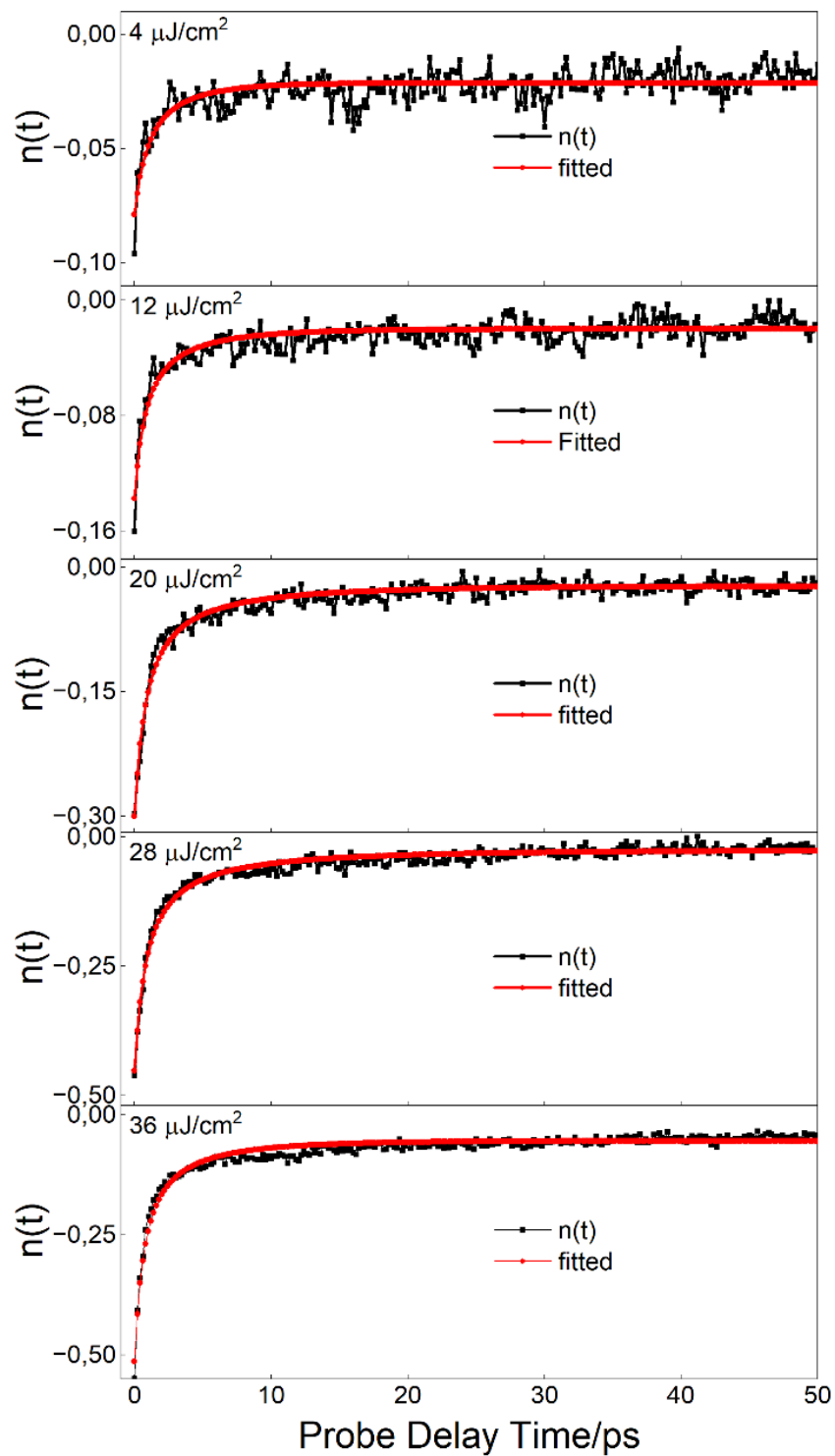


Fig. S6 Fitting results using the annihilation model for the differential transient transmission dynamics ($\Delta T/T$) obtained from the neat P3HT thin film at different excitation fluences where pump and probe both were at 638 nm.

5. Annihilation Rate

We have plotted the annihilation rate with the change of excitation fluence in Fig. S4. At higher excitation fluences, the annihilation rate is constant.

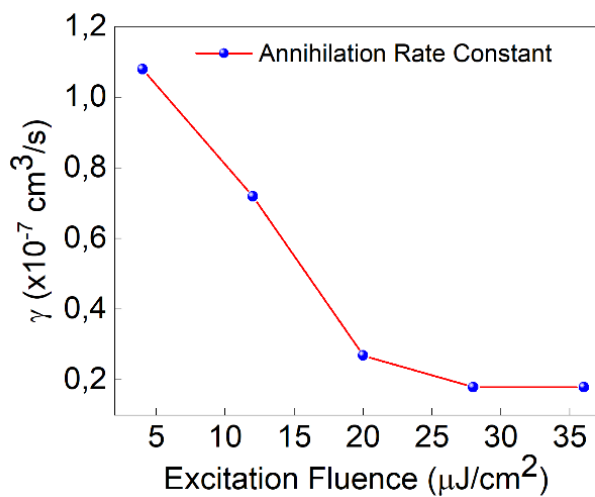


Fig. S7 Annihilation rate constant of delocalized polarons in neat P3HT thin film.

6. Fitting of Observed Dynamics

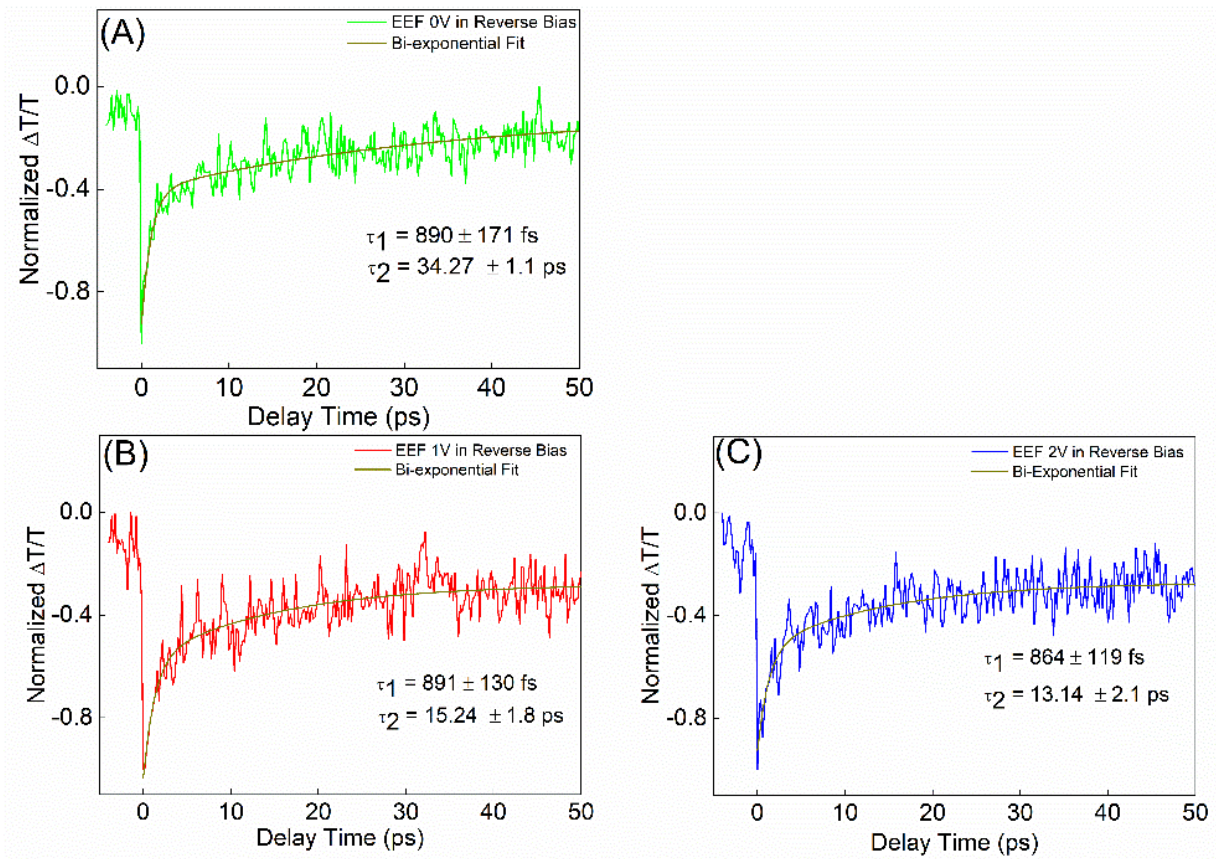


Fig. S8 Fitting results using the exponential model for the differential transient transmission dynamics ($\Delta T/T$) obtained from the P3HT device where the external electric field is varied. For the experiment, a pump excitation fluence of $4 \mu\text{J}/\text{cm}^2$ was chosen.

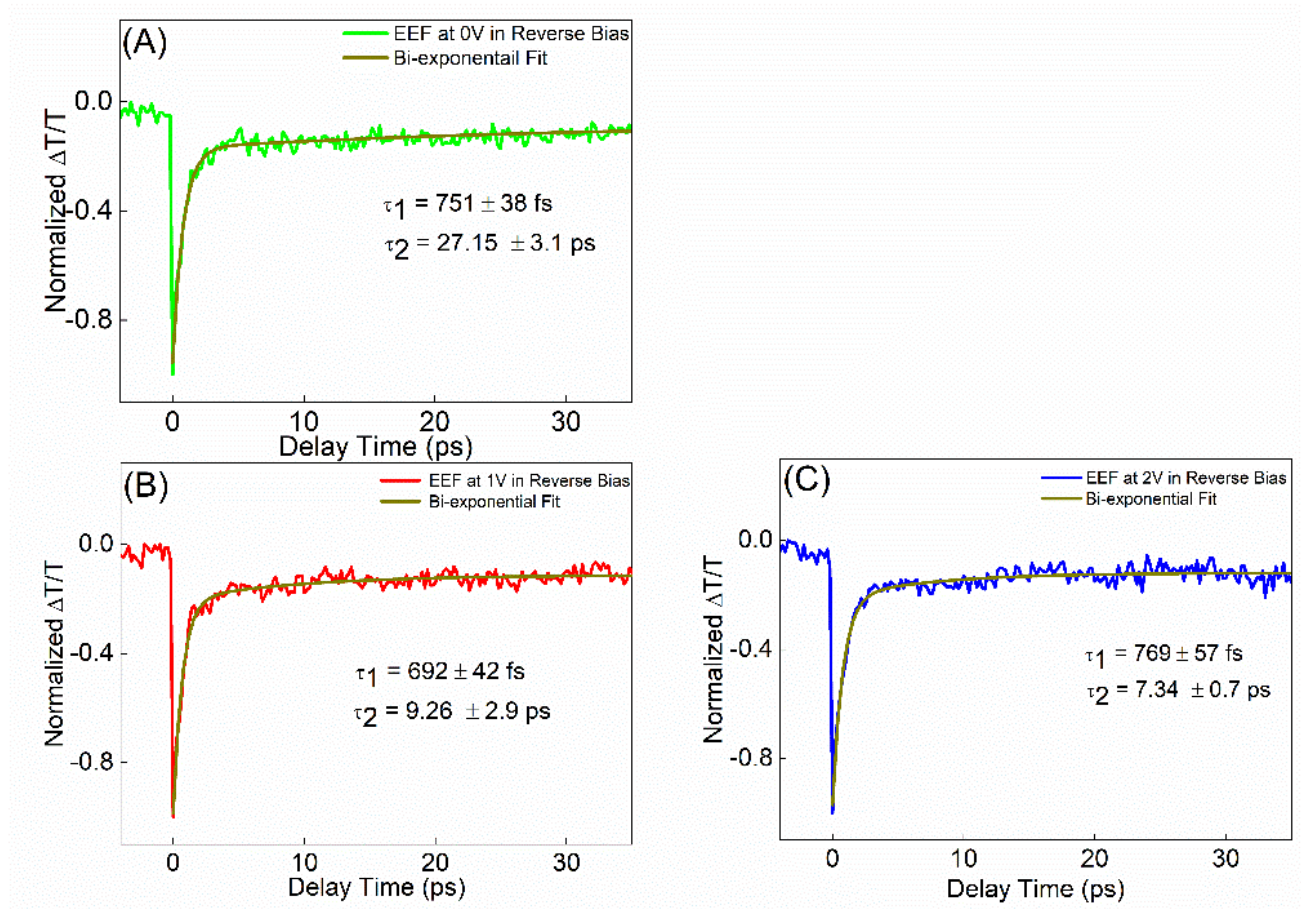


Fig. S9 Fitting results using the exponential model for the differential transient transmission dynamics ($\Delta T/T$) obtained from the P3HT device where the external electric field is varied. For the experiment, a pump excitation fluence of $20 \mu\text{J}/\text{cm}^2$ was chosen.

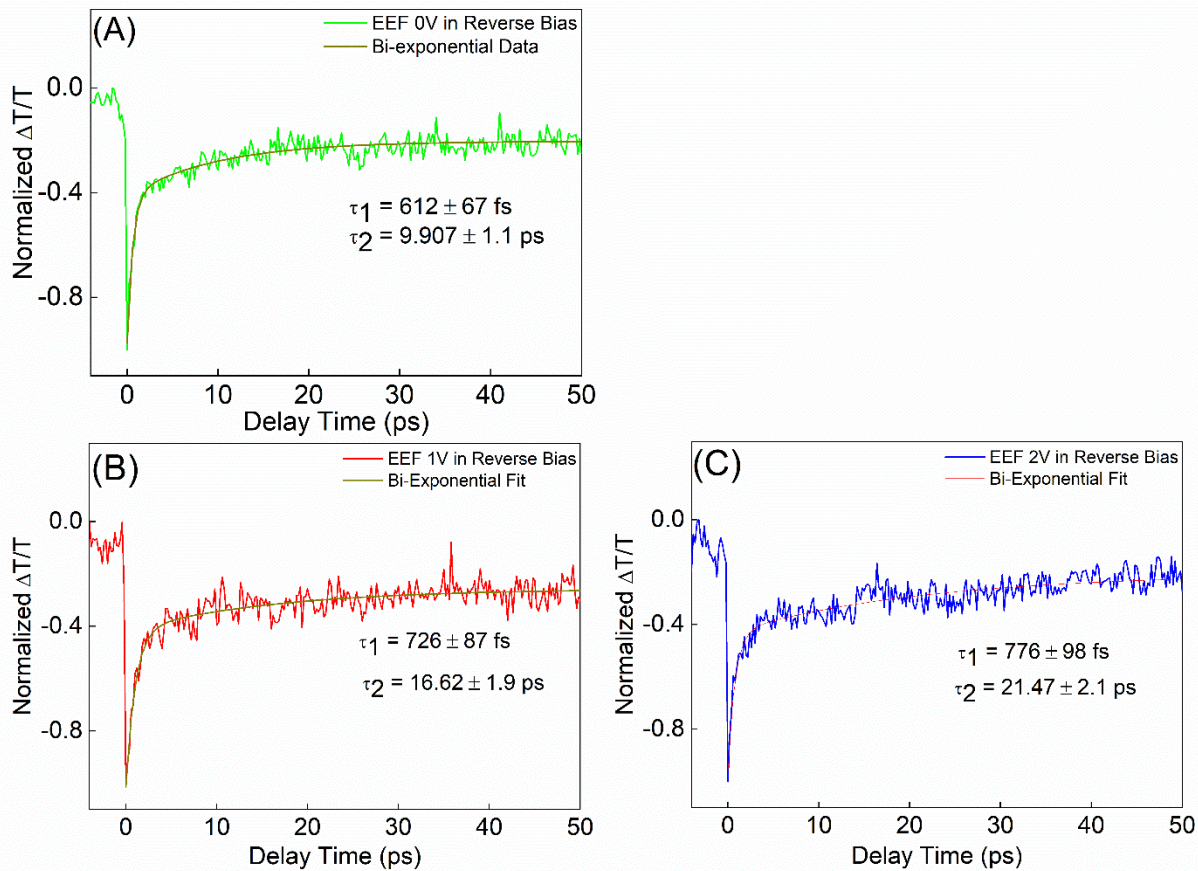


Fig. S10 Fitting results using the exponential model for the transient transmission dynamics ($\Delta T/T$) obtained from the P3HT device where the external electric field is varied. For the experiment, a pump excitation fluence of $28 \mu\text{J}/\text{cm}^2$ was chosen.

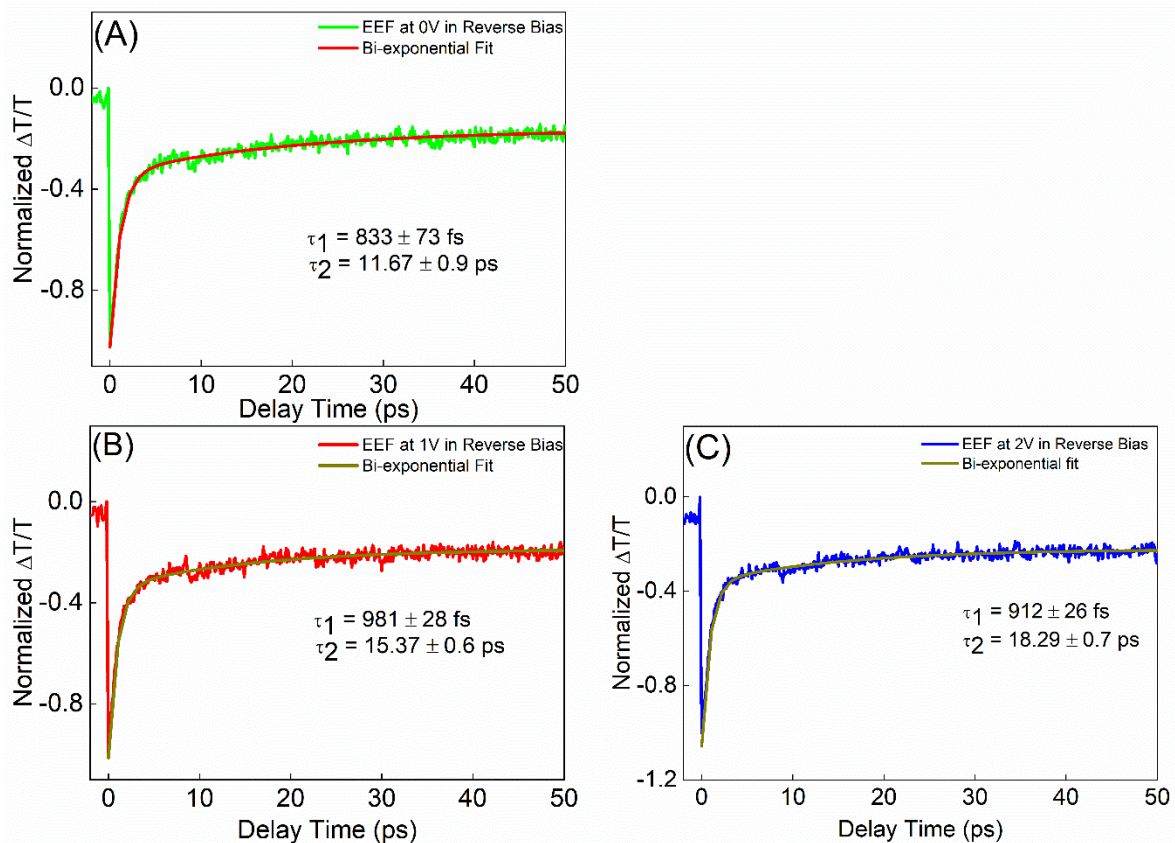


Fig. S11 Fitting results using the exponential model for the differential transient transmission dynamics ($\Delta T/T$) obtained from the P3HT device where the external electric field is varied. For the experiment, a pump excitation fluence of $36 \mu\text{J}/\text{cm}^2$ was chosen.

5. Fitting of Observed Dynamics Using Annihilation Model

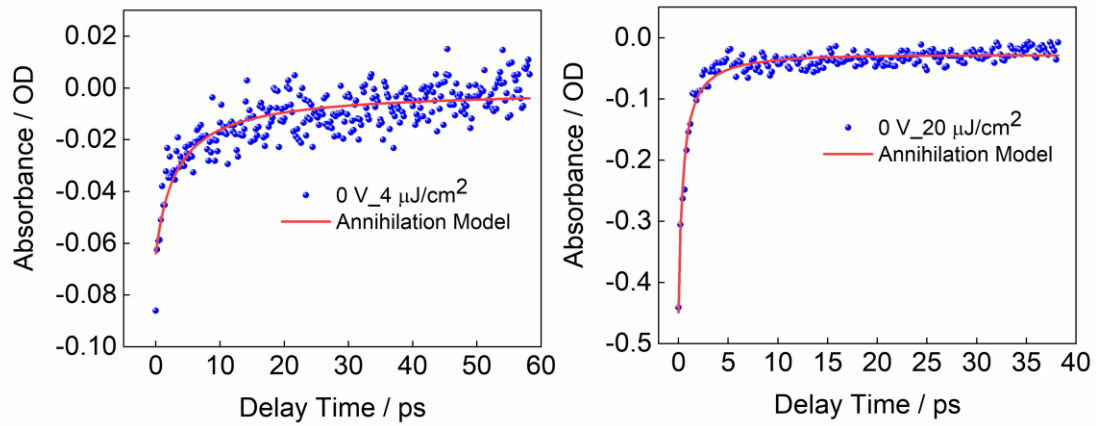


Fig. S12 Fitting results using the annihilation model for the differential transient transmission dynamics ($\Delta T/T$) obtained from the P3HT device where the external electric field is 0 V and hence only the built-in potential is present. For the experiment, a pump excitation fluence of 4 and 20 $\mu\text{J}/\text{cm}^2$ was chosen.

7. Fitting Parameters Obtained Using Annihilation Model

Table S1 The annihilation rate constants obtained for the neat P3HT diode for an external applied field in reverse bias with 0, -1, and -2 V (built-in-potential must be added) at different excitation fluences (compare plots in Fig. 6 (A) and (B)).

	4 $\mu\text{J}/\text{cm}^2$	20 $\mu\text{J}/\text{cm}^2$	28 $\mu\text{J}/\text{cm}^2$	36 $\mu\text{J}/\text{cm}^2$
0 V	$(4.41 \pm 0.015) \cdot 10^{-7}$	$(4.68 \pm 0.013) \cdot 10^{-7}$	$(3.87 \pm 0.011) \cdot 10^{-7}$	$(9.00 \pm 0.015) \cdot 10^{-8}$
-1 V	$(4.23 \pm 0.03) \cdot 10^{-7}$	$(4.59 \pm 0.015) \cdot 10^{-7}$	$(4.59 \pm 0.021) \cdot 10^{-7}$	$(9.00 \pm 0.013) \cdot 10^{-8}$
-2 V	$(4.14 \pm 0.02) \cdot 10^{-7}$	$(4.50 \pm 0.017) \cdot 10^{-7}$	$(4.68 \pm 0.016) \cdot 10^{-7}$	$(1.08 \pm 0.014) \cdot 10^{-8}$

Table S2 The dissociation time constants obtained for the neat P3HT diode for an external applied field in reverse bias with 0, -1, and -2 V (built-in-potential must be added) at different excitation fluences (compare plots in Fig. 6 (C) and (D)).

	4 $\mu\text{J}/\text{cm}^2$	20 $\mu\text{J}/\text{cm}^2$	28 $\mu\text{J}/\text{cm}^2$	36 $\mu\text{J}/\text{cm}^2$
0V	16.47 ± 0.11	6.68 ± 0.02	$6,64 \pm 0.02$	9.51 ± 0.02
-1V	15.74 ± 0.09	5.74 ± 0.01	$5,73 \pm 0.01$	8.02 ± 0.02
-2V	14.17 ± 0.06	5.68 ± 0.02	$5,68 \pm 0.01$	7.21 ± 0.02